Space-Time Signal Optimization for SWIPT: Linear Versus Nonlinear Energy Harvesting Model

Shuai Wang, Minghua Xia, and Yik-Chung Wu

***Abstract*— In simultaneous wireless information and power transfer systems, optimization of transmit signals is critical to system performance. Although the optimization problem can be efficiently solved under a linear energy harvesting model, the obtained solution may not work well in practice, since the energy harvester contains nonlinear elements, such as diodes. On the other hand, while a nonlinear model can be used to capture the dynamics of energy harvesting circuits, it introduces additional complexity at the optimization stage. Specifically, under a nonlinear model, traditional convex optimization is not applicable, since the energy harvesting function is fractional. To address this challenge, this letter first derives an optimal solution for static channels by introducing pseudo-inverse of the nonlinear model. Then, an iterative algorithm that converges to a sub-optimal solution is proposed for time varying channels. With the developed methods, the performance-complexity tradeoff between linear and nonlinear models is illustrated.**

***Index Terms*— SWIPT, nonlinear energy harvesting model, signal optimization, Internet of Things.**

I. Introduction

SIMULTANEOUS wireless information and power transfer (SWIPT) is widely accepted as a promising technique to prolong the lifetime of low-power consumption nodes in wireless sensor networks and Internet of Things [1]. However, a major difficulty to implement SWIPT systems in practice is the path-loss during power transfer. To combat the path-loss, transmit signal optimization becomes imperative, and the optimal signal design for SWIPT systems was extensively studied under a linear energy harvesting model [2] (i.e., by modelling the harvested direct-current (DC) power as a linear function of the incident radio frequency (RF) power).

Unfortunately, since the energy harvester contains nonlinear elements, such as diodes [3], linear energy harvesting model cannot accurately reflect the energy conversion process. To capture the dynamics of energy harvesting circuits, nonlinear models were recently proposed [4]–[6]. If the nonlinear model is concave (i.e., the constraint would be convex), the signal design can be handled by convex optimization [6]. Nonetheless, if the nonlinear model is not concave (which is true for most energy harvesting circuits), the method in [6] fails to work. To deal with this non-concave issue, sum of ratios programming was proposed in [5] for the signal design problem with one energy harvesting requirement. In the more general case with multiple energy harvesting requirements, however, the sum of ratios programming in [5] also becomes inapplicable.

To address the challenge brought by multiple non-convex constraints during signal optimization, this letter firstly derives an optimal solution for static channels by introducing pseudo-inverse of the nonlinear model. Then, a joint space-time signal design is created for time varying channels using an iterative algorithm, which is guaranteed to converge. Furthermore, a lower bound to the performance of the optimal signal design is derived based on a piece-wise linear function. With the newly developed algorithms, the power consumptions of SWIPT systems (based on the popular Powercast energy harvesting product P2110) under both linear and nonlinear models are simulated and compared. Our results show that the linear and nonlinear models perform similarly if the received powers are stable, whereas the nonlinear model is more preferable to the linear one if the received powers vary in a wide range. This results would provide insightful guidance on when we should use nonlinear models for signal optimization.

Notation: Italic letters, simple bold letters, and capital bold letters represent scalars, vectors, and matrices, respectively. The operators $\mathrm{Tr}(\cdot)$, $(\cdot)^T$, $(\cdot)^H$ take the trace, transpose, and Hermitian of a matrix, respectively. The operator $[x]^+ = \max(x, 0)$. Finally, $\mathbb{E}(\cdot)$ represents the expectation of a random variable and $\mathrm{e}^{(\cdot)}$ represents the exponential function of a scalar.

II. System Model and Problem Formulation

We consider a SWIPT system consisting of an access point with N antennas, K single-antenna energy harvesters (EHs), and L single-antenna information decoders (IDs).[1] During the downlink transmission, the access point delivers power to EHs and information to IDs within time duration T. To model the time varying feature of wireless channels, each time duration is further divided into M slots, and the channels are independent in different slots. At the m^{th} time slot ($1 \le m \le M$), the access point transmits a symbol $\mathbf{x}_m \in \mathbb{C}^{N\times 1}$ with covariance $\mathbf{X}_m = \mathbb{E}\left(\mathbf{x}_m \mathbf{x}_m^H\right) \in \mathbb{C}^{N\times N}$ and power $\mathrm{Tr}\left(\mathbf{X}_m\right)$.

Based on the above system model, the received signal at the l^{th} ID ($1 \le l \le L$) is given by $r_{l,m} = \mathbf{h}_{l,m}^H \mathbf{x}_m + n_{l,m}$, where $\mathbf{h}_{l,m}^H \in \mathbb{C}^{1\times N}$ is the downlink channel vector from the access point to the l^{th} ID and $n_{l,m}$ is the noise at the l^{th} ID. Based

[1] The energy harvesters and information decoders are separately located as in [2] and [5]. Furthermore, the derivations in this paper can be readily extended to multi-antenna users.

Manuscript received September 28, 2017; accepted October 27, 2017. Date of publication November 7, 2017; date of current version February 9, 2018. This work was supported by the National Natural Science Foundation of China (NSFC) under Grant No. 61671488, Special Fund for Science and Technology Development in Guangdong Province under Grants No. 2016A050503025 and No. 2016B010126003, and by the Fundamental Research Funds for the Central Universities of China under Grant No. 161gzd03. The associate editor coordinating the review of this paper and approving it for publication was K. E. Psannis. *(Corresponding author: Shuai Wang.)*

S. Wang and Y.-C. Wu are with the Department of Electrical and Electronic Engineering, The University of Hong Kong, Hong Kong (e-mail: swang@eee.hku.hk; ycwu@eee.hku.hk).

M. Xia is with the School of Electronics and Information Technology, Sun Yat-sen University, Guangzhou 510006, China (e-mail: xiamingh@mail.sysu.edu.cn).

Digital Object Identifier 10.1109/LCOMM.2017.2770142

on the expression of $r_{l,m}$, the data-rate achievable at the l^{th} ID is $\log_2\left(1+\text{Tr}\left(\mathbf{h}_{l,m}\mathbf{h}_{l,m}^H\mathbf{X}_m\right)/\sigma^2\right)$, with $\sigma^2=\mathbb{E}\left(|n_{l,m}|^2\right)$ being the noise power.

On the other hand, the received power at the k^{th} EH ($1\le k\le K$) is $\mathbb{E}\left(|\mathbf{g}_{k,m}^H\mathbf{x}_m|^2\right)=\text{Tr}\left(\mathbf{g}_{k,m}\mathbf{g}_{k,m}^H\mathbf{X}_m\right)$ provided that the thermal noise at the k^{th} EH is negligible compared with that of $\mathbf{x}_m$, where $\mathbf{g}_{k,m}^H\in\mathbb{C}^{1\times N}$ is the downlink channel vector from access point to the k^{th} EH. Accordingly, the harvested power is denoted by $\Upsilon\Big(\text{Tr}\left(\mathbf{g}_{k,m}\mathbf{g}_{k,m}^H\mathbf{X}_m\right)\Big)$, where Υ is the function representing the RF-DC energy conversion process.

In SWIPT systems, a main task is to guarantee sufficient harvested power at EHs and provide reliable communications for the IDs. Having the energy harvesting and data-rate requirements satisfied, it is then crucial to minimize the power consumption at the access point, and an optimization problem can be formulated as:

$$\text{P1}\quad \min_{\{\mathbf{X}_m\succeq 0\}}\ \frac{1}{M}\sum_{m=1}^{M}\text{Tr}(\mathbf{X}_m)$$

$$\text{s.t. }\frac{1}{M}\sum_{m=1}^{M}\Upsilon\Big(\text{Tr}\left(\mathbf{g}_{k,m}\mathbf{g}_{k,m}^H\mathbf{X}_m\right)\Big)\ge\gamma_k,\quad\forall k \tag{1a}$$

$$\frac{1}{M}\sum_{m=1}^{M}\log_2\left(1+\frac{1}{\sigma^2}\text{Tr}\Big(\mathbf{h}_{l,m}\mathbf{h}_{l,m}^H\mathbf{X}_m\Big)\right)\ge\theta_l,\quad\forall l. \tag{1b}$$

III. Energy Harvesting Models

Before we solve P1, we need to specify the energy conversion function Υ, which unfortunately does not have a closed-form expression and can only be obtained numerically, e.g., using look-up tables [7]. To address this issue, we need a tractable model to approximate Υ. Since $P_{\text{out}}=\Upsilon(P_{\text{in}})$ is a monotonic increasing function of input power P_{in}, a straightforward way is to adopt a linear model $\Upsilon_{\text{linear}}(P_{\text{in}})=\eta P_{\text{in}}$ [2], where η is a constant representing the energy harvesting efficiency.

On the other hand, as the energy harvester contains nonlinear elements, the efficiency η is not a constant in practice. In fact, as the input power P_{in} rises, η should increase to a maximum value and then decrease [7], which indicates that the function Υ should behave like an "S" curve. To represent this curve, a logistic model was proposed in [5] as

$$\Upsilon_{\text{nl}}(P_{\text{in}})=\left[\frac{P_{\max}}{\text{e}^{-\tau P_0+\nu}}\left(\frac{1+\text{e}^{-\tau P_0+\nu}}{1+\text{e}^{-\tau P_{\text{in}}+\nu}}-1\right)\right]^+,$$

where the parameter P_0 denotes the harvester's sensitivity threshold (which was set to zero in [5]) and $P_{\max}$ refers to the maximum harvested power when the energy harvesting circuit is saturated [5]. Moreover, the parameters τ and ν are used to capture the nonlinear dynamics of energy harvesting circuits.

IV. Space-Time Signal Optimization

If Υ is approximated as Υ_{linear}, the constraint defined in (1a) becomes $\frac{1}{M}\sum_{m=1}^{M}\eta\text{Tr}\left(\mathbf{g}_{k,m}\mathbf{g}_{k,m}^H\mathbf{X}_m\right)\ge\gamma_k$. Based on the above procedure, P1 becomes a convex problem which can be solved by CVX MOSEK, a popular software package for solving convex problems [8]. Since $\{\mathbf{X}_m\}$ are involved in M semidefinite constraints of dimension $N\times N$, K linear constraints, and ML linear terms, the complexity for solving P1 under the linear model is $O\Big[(MN)^{0.5}(K+ML)\Big((K+ML)^2+(K+ML)MN^2+MN^3\Big)\Big]$ [9].

On the other hand, if Υ is approximated as Υ_{nl}, multiple fractional constraints are involved in (1a). In such a case, traditional methods like convex optimization in [2] and sum-of-ratios programming in [5] are not applicable. To tackle this challenge, in the following, we first provide an optimal solution in the case of $M=1$, and then provide an iterative solution for the general case of $M\ge 2$.

A. Optimal Solution for the Case of $M=1$

In the case of $M=1$, the subscript m can be dropped to simplify the notation and the constraint (1a) reduces to $\Upsilon_{\text{nl}}\Big(\text{Tr}\left(\mathbf{g}_k\mathbf{g}_k^H\mathbf{X}\right)\Big)\ge\gamma_k$. From this equivalent constraint, we consider two cases as follows.

(i) If $\gamma_k\ge P_{\max}$, the constraint (1a) would always be infeasible, since the function value of Υ_{nl} is upper bounded by $P_{\max}$. In such a case, we simply write (1a) as $\text{Tr}(\mathbf{g}_k\mathbf{g}_k^H\mathbf{X})\to\infty$.

(ii) If $0<\gamma_k<P_{\max}$, the operator $[\cdot]^+$ in (1a) can be dropped. By further solving for $\text{Tr}(\mathbf{g}_k\mathbf{g}_k^H\mathbf{X})$, we get

$$\text{Tr}(\mathbf{g}_k\mathbf{g}_k^H\mathbf{X})\ge\underbrace{\frac{\nu}{\tau}-\frac{1}{\tau}\ln\Big(\frac{1+\text{e}^{-\tau P_0+\nu}}{1+P_{\max}^{-1}\text{e}^{-\tau P_0+\nu}\gamma_k}-1\Big)}_{:=A(\gamma_k)}.$$

Combining (i)-(ii), problem P1 can be reformulated as

$$\begin{aligned}\text{P2}\quad&\min_{\{\mathbf{X}\succeq 0\}}\ \text{Tr}(\mathbf{X})\\&\text{s.t. }\text{Tr}(\mathbf{g}_k\mathbf{g}_k^H\mathbf{X})\ge\Upsilon_{\text{nl}}^{\dagger}(\gamma_k),\quad\forall k\\&\qquad\text{Tr}(\mathbf{h}_l\mathbf{h}_l^H\mathbf{X})\ge\left(2^{\theta_l}-1\right)\sigma^2,\quad\forall l,\end{aligned}$$

where $\Upsilon_{\text{nl}}^{\dagger}(\gamma_k)=+\infty$ if $\gamma_k\ge P_{\max}$ and $\Upsilon_{\text{nl}}^{\dagger}(\gamma_k)=A(\gamma_k)$ if $0<\gamma_k<P_{\max}$, and the second constraint of P2 is obtained from (1b). Now P2 is a semi-definite programming problem and can be optimally solved using CVX with a complexity of $O\Big[N^{0.5}\Big((K+L)^3+(K+L)^2N^2+(K+L)^3N^3\Big)\Big]$ [9].

B. Joint Space-Time Signal Design for the Case of $M\ge 2$

If $M\ge 2$, solving P1 is difficult due to the sum of fractional functions. However, by observing that the denominator of Υ_{nl} involves exponential functions, we may introduce slack variables $\{\lambda_{k,m}\}$ such that $\lambda_{k,m}=\text{e}^{\tau\text{Tr}\left(\mathbf{g}_{k,m}\mathbf{g}_{k,m}^H\mathbf{X}_m\right)}$ for all k,m. With the above slack variables, the constraint (1a) can be rewritten as

$$\frac{1}{M}\sum_{m=1}^{M}\underbrace{\left[\frac{P_{\max}}{\text{e}^{-\tau P_0+\nu}}\left(\frac{1+\text{e}^{-\tau P_0+\nu}}{1+\text{e}^{\nu}/\lambda_{k,m}}-1\right)\right]^+}_{:=\Phi(\lambda_{k,m})}\ge\gamma_k, \tag{2}$$

and $\Phi(\lambda_{k,m})$ can be reformulated as

$$\Phi(\lambda_{k,m}) = \frac{P_{\max}(1+\mathrm{e}^{-\tau P_0+\nu})}{\mathrm{e}^{-\tau P_0+\nu}} - \frac{P_{\max}}{\mathrm{e}^{-\tau P_0+\nu}} - \frac{P_{\max}(1+\mathrm{e}^{-\tau P_0+\nu})}{\mathrm{e}^{-\tau P_0+\nu}} \times \frac{\mathrm{e}^{\nu}}{\lambda_{k,m}+\mathrm{e}^{\nu}}. \quad (3)$$

Since the term $\frac{\mathrm{e}^{\nu}}{\lambda_{k,m}+\mathrm{e}^{\nu}}$ is convex, $-\frac{\mathrm{e}^{\nu}}{\lambda_{k,m}+\mathrm{e}^{\nu}}$ is concave. As a consequence, $\Phi(\lambda_{k,m})$ is concave. On the other hand, we can relax $\lambda_{k,m} = \mathrm{e}^{\tau \mathrm{Tr}\left(\mathbf{g}_{k,m}\mathbf{g}_{k,m}^H \mathbf{X}_m\right)}$ into

$$\lambda_{k,m} \le \mathrm{e}^{\tau \mathrm{Tr}\left(\mathbf{g}_{k,m}\mathbf{g}_{k,m}^H \mathbf{X}_m\right)}. \quad (4)$$

As proved in Appendix A, the solution of the relaxed problem is optimal to the original problem, and thus the relaxation can be safely applied.

After the above procedure, the remaining obstacle in (2) is the operators $[\cdot]^+$. Fortunately, since $[x]^+ = \max(x, 0) \ge x$, dropping the operators $[\cdot]^+$ would make the feasible set of (2) smaller and the solution of such a problem would be feasible for P1. To this end, P1 becomes

$$\mathrm{P3} \quad \min_{\{\mathbf{X}_m \succeq 0, \lambda_{k,m} \ge 1\}} \frac{1}{M}\sum_{m=1}^{M} \mathrm{Tr}(\mathbf{X}_m)$$

$$\text{s.t. } \tau \mathrm{Tr}(\mathbf{g}_{k,m}\mathbf{g}_{k,m}^H \mathbf{X}_m) \ge \ln(\lambda_{k,m}), \quad \forall k, m \quad (5a)$$

$$\frac{1}{M}\sum_{m=1}^{M} \Phi(\lambda_{k,m}) \ge \gamma_k, \quad \forall k \quad (5b)$$

$$\frac{1}{M}\sum_{m=1}^{M} \log_2\left(1+\frac{\mathrm{Tr}(\mathbf{h}_{l,m}\mathbf{h}_{l,m}^H \mathbf{X}_m)}{\sigma^2}\right) \ge \theta_l, \quad \forall l. \quad (5c)$$

where the first constraint is obtained from (4). Now the only nonconvex part in P3 is $\Xi(\lambda_{k,m}) := \ln(\lambda_{k,m})$ in (5a). Since $\ln(\lambda_{k,m})$ is concave, we can apply the inner approximation method [10] to replace $\Xi(\lambda_{k,m})$ with its first-order approximation around a feasible point. In particular, given any feasible point $\{\lambda_{k,m}^\star\}$ of P3, we define a surrogate function $\tilde{\Xi}$ as $\tilde{\Xi}(\lambda_{k,m}|\lambda_{k,m}^\star) = \ln(\lambda_{k,m}^\star) + \frac{\lambda_{k,m}}{\lambda_{k,m}^\star} - 1$. Due to the concave property of $\Xi(\lambda_{k,m})$, we immediately have $\tilde{\Xi}(\lambda_{k,m}|\lambda_{k,m}^\star) \ge \Xi(\lambda_{k,m})$. Therefore, if we replace the function Ξ by $\tilde{\Xi}$ expanded around $\{\lambda_{k,m}^\star\}$, the solution of the surrogate problem is also feasible for P3. By treating the obtained solution as another feasible point and continue to construct the next round surrogate functions, we can improve the solution iteratively. In particular, assuming that the solution at the n^{th} iteration is given by $\{\mathbf{X}_m^{[n]}, \lambda_{k,m}^{[n]}\}$, the following problem is considered at the $(n+1)^{\text{th}}$ iteration:

$$\mathrm{P3}[n+1] \quad \min_{\{\mathbf{X}_m \succeq 0, \lambda_{k,m} \ge 1\}} \frac{1}{M}\sum_{m=1}^{M} \mathrm{Tr}(\mathbf{X}_m)$$

$$\text{s.t. } \tau \mathrm{Tr}(\mathbf{g}_{k,m}\mathbf{g}_{k,m}^H \mathbf{X}_m) \ge \tilde{\Xi}(\lambda_{k,m}|\lambda_{k,m}^{[n]}), \quad \forall k, m$$
$$(5b) - (5c).$$

Problem P3$[n+1]$ is a convex problem and can be optimally solved. Denoting its optimal solution as $\left\{\mathbf{X}_m^*, \lambda_{k,m}^*\right\}$, then we can set $\left\{\mathbf{X}_m^{[n+1]} = \mathbf{X}_m^*, \lambda_{k,m}^{[n+1]} = \lambda_{k,m}^*\right\}$, and the process repeats with solving the problem P3$[n+2]$. The entire procedure is summarized as Algorithm 1 and the following property (proved in Appendix B) can be established.

Property 1: Algorithm 1 converges to a Karush-Kuhn-Tucker solution of P3.

While *Property 1* indicates that the converged point $\{\mathbf{X}_m^\diamond\}$ generated by Algorithm 1 is a Karush-Kuhn-Tucker (KKT) solution of P3, $\{\mathbf{X}_m^\diamond\}$ is not necessarily a KKT solution of P1. As a result, the proposed Algorithm 1 is a sub-optimal method for solving P1. However, as shown later in the simulations, the performance of Algorithm 1 is very close to the lower bound of P1, showing that Algorithm 1 provides a good solution in practice. In terms of computational complexity, Algorithm 1 requires a complexity of $O\Big[Q(MN)^{0.5}(K+ML)\Big((K+ML)^2+(K+ML)MN^2+MN^3\Big)\Big]$, where Q is the number of iterations for the algorithm to converge.

Algorithm 1 Joint Space-Time Signal Design

1: **Initialize** a feasible $\left\{\mathbf{X}_m^{[0]}, \lambda_{k,m}^{[0]}\right\}$ of P3 and set $n = 0$.
2: **Repeat**
3: Solve P3$[n+1]$ and update $\left\{\mathbf{X}_m^{[n+1]}, \lambda_{k,m}^{[n+1]}\right\}$.
4: Set $n = n + 1$.
5: **Until** convergence. The converged point is $\left\{\mathbf{X}_m^\diamond, \lambda_{k,m}^\diamond\right\}$.

C. Performance Lower Bound

To evaluate the optimization performance brought by adopting Υ_{linear} and Υ_{nl}, we need a performance lower bound for P1. Accordingly, we propose to use a piecewise linear function $\min(\beta x, P_{\max})$ to bound Υ from above. To choose β such that $\min(\beta x, P_{\max})$ is as tight as possible, the following problem is considered:

$$\min_{\beta} \ \beta \quad \text{s.t. } \min(\beta x, P_{\max}) \ge \Upsilon(x), \quad \forall x \ge 0. \quad (6)$$

Due to $P_{\text{out}} \ge 0$ and $P_{\text{out}} \le P_{\text{in}}$, β is bounded within $0 \le \beta \le 1$. Moreover, it can be seen that the above problem only has one scalar variable β. Therefore, a bisection search algorithm can be applied within the interval $[0, 1]$, and the optimal solution is denoted as β^*. Replacing $\Upsilon\left(\mathrm{Tr}\left(\mathbf{g}_{k,m}\mathbf{g}_{k,m}^H \mathbf{X}_m\right)\right)$ with $\min\left(\beta^* \mathbf{g}_{k,m}\mathbf{g}_{k,m}^H \mathbf{X}_m, P_{\max}\right)$ in P1, the modified problem is convex and can be optimally solved by CVX MOSEK.

V. Simulation Results and Discussions

This section provides simulation results to compare the linear and nonlinear energy harvesting models. In particular, the number of antennas is set to $N = 16$ and the noise powers are $\sigma^2 = -50$ dBm (corresponding to power spectral density -120 dBm/Hz with 10 MHz bandwidth). The data-rate requirements are set to $\theta_1 = \cdots = \theta_L = 5$ in bps/Hz, and the look-up table function Υ is obtained from Powercast data sheet of energy harvester P2110 [3]. Based on Υ, the parameters in the nonlinear model are obtained by fitting the experimental data of Υ to the model, and they are given by $\tau = 274$, $\nu = 0.29$, $P_{\max} = 4.927$ mW

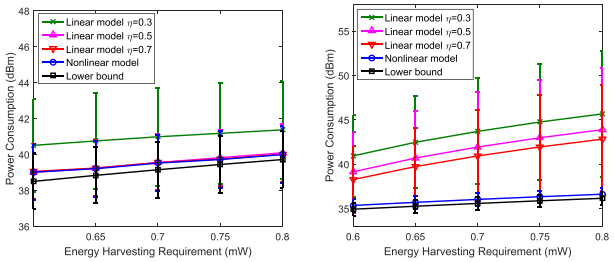

Fig. 1. Power consumption versus energy harvesting requirement in the case of (a) $M = 1$ and $K = L = 2$; (b) $M = 10$ and $K = L = 2$. The vertical lines indicate the 95% confidence intervals.

and $P_0 = 0.064$ mW. Since the received powers at EHs are not known a prior, the energy harvesting efficiency η in the linear model is also not known, and in this letter we choose $\eta \in \{0.3, 0.5, 0.7\}$. Furthermore, using the method in Section IV-C, we can compute the lower bound parameter $\beta^* = 0.5518$. Notice that a feasible solution under the model Υ_{linear} or Υ_{nl} may not be feasible under the real conversion process Υ [3]. As a result, the obtained solutions need to be scaled such that all the EH requirements are satisfied under the function Υ.

On the other hand, the path-loss model $\rho_k = \rho_0 \cdot (\frac{d_u}{d_0})^{-\alpha}$ is adopted, where d_k is the distance from the k^{th} EH to the access point, $\rho_0 = 10^{-3}$, $d_0 = 1$ m, and α is the path-loss exponent set to 2.7 [1]. The distances are set to $d_k \sim \mathcal{U}(1, 5)$ in the unit of meters for EHs, where $\mathcal{U}$ denotes the uniform distribution. Based on the path-loss model, $\mathbf{g}_{k,m}$ is generated according to $\mathcal{CN}(\mathbf{0}, \rho_k \mathbf{I})$. Following a similar procedure and by setting the distances as $\mathcal{U}(10, 50)$ for IDs, channels $\{\mathbf{h}_{l,m}\}$ can be generated. Each point in the figures is obtained by averaging over 100 simulation runs, with independent channels between consecutive runs.

With the energy harvesting and path-loss models, we first consider the case of $M = 1$ with $K = L = 2$. It can be observed from Fig. 1a that with η properly chosen for the linear model, the power consumptions based on linear and nonlinear models are similar. This is because the received powers at EHs are stable and the linear model can be locally accurate. However, since the appropriate η may vary under different system setups, we need to try different values of η for the linear model and this searching procedure would increase the complexity of signal optimization. In contrast, the signal designs under the nonlinear model can automatically adjust the efficiency and do not require such a searching procedure.

Next, we consider the case of $M = 10$ with $K = L = 2$. It can be observed from Fig. 1b that the nonlinear model achieves a transmit power close to the lower bound and brings significant performance gain compared to the linear model. This is because the received powers at EHs vary in a wide range during different time slots and a constant η in the linear model cannot represent the time-varying energy harvesting efficiency. Moreover, it can be seen from Fig. 1b that the variances of transmit powers based on nonlinear models are significantly smaller, which indicates that the nonlinear models lead to more stable performance in time-varying channels. Therefore, a nonlinear model is necessary when the fluctuation of received power is significant.

VI. Conclusions

This letter studied the signal optimization in SWIPT systems under linear and nonlinear energy harvesting models. In particular, efficient algorithms were proposed under both models. Adopting the developed algorithms, it was found that the linear and nonlinear models lead to similar performance if the received powers are stable and the parameter in the linear model is properly tuned. However, the nonlinear model results in a significantly lower power consumption than the linear model if the received powers vary in a wide range.

Appendix A

To prove that the relaxation would not change the solution, we first compute

$$\nabla \Phi(\lambda_{k,m}) = \frac{P_{\max}(1 + \mathrm{e}^{-\tau P_0 + \nu})}{\mathrm{e}^{-\tau P_0 + \nu}} \cdot \frac{\mathrm{e}^{\nu}}{(\lambda_{k,m} + \mathrm{e}^{\nu})^2} \geq 0.$$

It can be seen from the above equation that $\Phi(\lambda_{k,m})$ is a monotonically increasing function. Therefore, we can always increase $\lambda_{k,m}$ to activate the constraint (4) without violating the constraint (2). This indicates that there always exist an optimal $\lambda^*_{k,m}$ of the relaxed problem that activates the constraint (4), which completes the proof.

Appendix B

To prove the property, we first compute

$$\tilde{\Xi}(\lambda^{\diamond}_{k,m} | \lambda^{\diamond}_{k,m}) = \ln(\lambda^{\diamond}_{k,m}) = \Xi(\lambda^{\diamond}_{k,m}),$$

$$\frac{\partial \tilde{\Xi}(\lambda_{k,m} | \lambda^{\diamond}_{k,m})}{\partial \lambda_{k,m}}\Big|_{\lambda_{k,m} = \lambda^{\diamond}_{k,m}} = \frac{1}{\lambda^{\diamond}_{k,m}} = \frac{\partial \Xi(\lambda_{k,m})}{\partial \lambda_{k,m}}\Big|_{\lambda_{k,m} = \lambda^{\diamond}_{k,m}}.$$

Using the above results and based on [10, Th. 1], Algorithm 1 must converge to a KKT solution of P3.

References

[1] M. Xia and S. Aïssa, "On the efficiency of far-field wireless power transfer," *IEEE Trans. Signal Process.*, vol. 63, no. 11, pp. 2835–2847, Jun. 2015.

[2] R. Zhang and C. K. Ho, "MIMO broadcasting for simultaneous wireless information and power transfer," *IEEE Trans. Wireless Commun.*, vol. 12, no. 5, pp. 1989–2001, May 2013.

[3] (Nov. 2016). *Powercast Wireless Power Calculator*. [Online]. Available: http://www.powercastco.com/power-calculator/

[4] Y. Dong, M. J. Hossain, and J. Cheng, "Performance of wireless powered amplify and forward relaying over Nakagami-*m* fading channels with nonlinear energy harvester," *IEEE Commun. Lett.*, vol. 20, no. 4, pp. 672–675, Apr. 2016.

[5] E. Boshkovska, D. W. K. Ng, N. Zlatanov, and R. Schober, "Practical non-linear energy harvesting model and resource allocation for SWIPT systems," *IEEE Commun. Lett.*, vol. 19, no. 12, pp. 2082–2085, Dec. 2015.

[6] E. Boshkovska, D. W. K. Ng, N. Zlatanov, A. Koelpin, and R. Schober, "Robust resource allocation for MIMO wireless powered communication networks based on a non-linear EH model," *IEEE Trans. Commun.*, vol. 65, no. 5, pp. 1984–1999, May 2017.

[7] C. R. Valenta and G. D. Durgin, "Harvesting wireless power: Survey of energy-harvester conversion efficiency in far-field, wireless power transfer systems," *IEEE Microw. Mag.*, vol. 15, no. 4, pp. 108–120, Jun. 2014.

[8] S. Boyd and L. Vandenberghe, *Convex Optimization*. Cambridge, U.K.: Cambridge Univ. Press, 2004.

[9] A. Ben-Tal and A. Nemirovski, *Lectures on Modern Convex Optimization* (MPS/SIAM Series on Optimizations). Philadelphia, PA, USA: SIAM, 2013.

[10] B. R. Marks and G. P. Wright, "A general inner approximation algorithm for nonconvex mathematical programs," *Oper. Res.*, vol. 26, no. 4, pp. 681–683, Jul. 1978.